Differential Scattering Cross Sections for $HeCl_2$, $NeCl_2$, and $ArCl_2$: Multiproperty Fits of the Potential Energy Surfaces

Andreas Rohrbacher and Kenneth C. Janda*

Department of Chemistry and Institute for Surface and Interface Science, University of California, Irvine, California 92697-2025

Laura Beneventi, Piergiorgio Casavecchia, and Gian Gualberto Volpi

Dipartimento di Chimica, Universitá di Perugia, 06100 Perugia, Italy

Received: February 27, 1997; In Final Form: May 30, 1997[⊗]

Differential scattering cross section measurements are reported for the Ne and Ar scattering from Cl_2. This new data, along with previously published data and *ab initio* quantum calculations, are used to determine potential energy surfaces for $HeCl_2$, $NeCl_2$, and $ArCl_2$ via multiproperty fits. The starting point of the fitting procedure was fitting a one-center Morse-spline-van der Waals potential to a set of *ab initio* points for each molecule. Because the resulting *ab initio* potential is highly anisotropic, this fit required the use of up to nine anisotropy parameters, many more than could independently be fitted with experimental data alone. Therefore the *ab initio* potential was adjusted to fit the data by varying as few of the parameters as possible. The fit to the scattering data was carried out within the infinite order sudden approximation. The fits were also constrained by spectroscopically determined rotational constants and experimental dissociation energies (except for $HeCl_2$ for which no measurement of D_0 is available). These were calculated from the potentials via a *J*-dependent variational method. The *ab initio* surfaces can be brought into good accord with the data by an overall deepening of the potentials and a slight shift to shorter distances. In the case of $NeCl_2$, for which the best data is available, no changes in the anisotropy parameters were necessary to achieve an excellent fit. For $HeCl_2$ and $ArCl_2$ the fitting required slightly more adjustments, and there are more uncertainties inherent in the fitting method, but very good agreement is still achieved. The present multiproperty analysis confirms that the highly anisotropic *ab initio* surfaces, with similar well depths for the linear and perpendicular configurations, are consistent with the experimental data. We believe that these are the best available surfaces for the ground states of these molecules, and that new data or much higher level calculations will be required to achieve significant improvements.

I. Introduction

Given the numerous studies that have investigated the behavior of halogen molecules in contact with noble gas atoms, it is surprising that there is still no agreement regarding even the qualitative shape of the noble gas−halogen potential for the ground electronic state. Within the last several years, a wide variety of potentials have been published. The goal of this paper is to use all of currently available information to determine the intermolecular potentials for $HeCl_2$, $NeCl_2$, and $ArCl_2$. New differential scattering cross section (DCS) data is reported for $NeCl_2$ and $ArCl_2$. This data, along with previously reported DCS data for $HeCl_2$, is combined with spectroscopic data for the rotational constants and dissociation energies (except that no D_0 is available for $HeCl_2$) to constrain a fit to the potentials. In each case, the starting point of the fit was a set of *ab inito* points. The *ab initio* surfaces could be adjusted to fit the experimental data by lowering the overall well depths by 5−24% and shortening the well distances slightly. For $NeCl_2$, for which the most comprehensive data is available, these minor changes were enough to achieve excellent fits. For $HeCl_2$ and $ArCl_2$ very slight changes in the anisotropy parameters were necessary to achieve the desired fit quality. We believe that the potentials obtained here are the best that can be obtained with currently available information. We are very happy to present this work in this special issue of *The Journal of Physical Chemistry B* in honor of Professor Y. T. Lee, who has had such a profound impact on the methodology used to study molecular physics. Of course, fitting potentials is always a somewhat risky business since there is no unique fit, and any fit depends on the fitting function that is chosen. These issues are discussed in some detail. We start with a brief review of the type of data that is currently available on these systems.

A laser-induced fluorescence (LIF) spectrum of $HeCl_2$ was first obtained by Janda and co-workers.[1] Pump−probe spectroscopy was done on the same molecule and yielded information on the dynamics.[2,3] The differential scattering cross section of the He + Cl_2 system was studied together with spectroscopic data by Beneventi *et al.*[4] and was further analyzed by Huang *et al.*[5] Among the theoretical studies of $HeCl_2$ is the work of Reid *et al.*,[6] who employed realistic intramolecular potentials to calculate rovibrational energy levels and wavefunctions. *Ab initio* calculations for the X electronic state potential energy surface of $HeCl_2$ were performed by Chałasiński *et al.*[7] and by Tao and co-workers.[8] The B electronic state of $HeCl_2$ was studied by Rohrbacher *et al.*,[9] who employed a Cl−Cl distance dependent *ab initio* potential energy surface for the B state to calculate an excitation spectrum and several dynamical properties. A diatomics-in-molecules (DIM) approach for $HeCl_2$ (and $ArCl_2$) was taken by Grigorenko *et al.*[10] who included ion-pair states in the description of the potential energy surfaces and discussed the stability of the T-shaped and linear isomers.

$NeCl_2$ was first observed by Brinza *et al.*[11,12] They also observed vibrationally excited $NeCl_2$ molecules, which is

[⊗] Abstract published in *Advance ACS Abstracts,* August 1, 1997.

S1089-5639(97)00738-X CCC: $14.00

TABLE 1: Beam Parameters

	He		Ne	Ar	Cl_2
nozzle diameter (mm)	0.025	0.025	0.025	0.025	0.10
source pressure (bar)	48	26	18	4	0.5
source temperature (K)	308	97.5	302	302	315
peak velocity (m/s)	1786	1005	792	559	503
speed ratio	44.7	49.6	36.0	24.5	7.8
$\Delta v/v$ (%)	3.7	3.3	4.6	6.7	21
beam divergence (deg)	0.4	0.4	0.4	0.4	1.8
skimmer diameter (mm)	0.50	0.50	0.50	0.50	0.65
distance nozzle−skimmer (mm)	9.5	9.5	9.5	9.5	6.3
distance nozzle−collision center (mm)	86	86	86	86	57

interesting, because the Cl−Cl vibrational energy far exceeds the Ne−Cl_2 bond energy. A high-resolution LIF spectrum was obtained by the same group[13] and used to improve the spectral constants of $NeCl_2$. Vibrational predissociation lifetimes for several vibrational states of $NeCl_2$ were obtained by Evard *et al.*[14] and analyzed in terms of momentum gap arguments. Pump−probe spectra were obtained by Cline *et al.*[15] and used to determine the rotational product state distribution for the vibrational predissociation of $NeCl_2$. Theoretical studies include the work of Halberstadt *et al.*,[16] who did three-dimensional quantum mechanical calculations on the $NeCl_2$ vibrational predissociation and compared the results to experimental data. Tao and co-workers[8] carried out *ab initio* calculations for $NeCl_2$. Very recently, Buchachenko *et al.*[17] used diatom-in-molecule (DIM) potentials to describe various properties of $NeCl_2$.

For $ArCl_2$ several experimental and theoretical studies have also been reported. Janda and co-workers[18] measured a pump−probe optical spectrum of this van der Waals complex and determined the structural parameters and the bond energy. A microwave spectrum of $ArCl_2$ was measured by Xu *et al.*[19] and yielded greatly improved rotational constants for the ground electronic state. In 1992 Tao and Klemperer[20] calculated a potential energy surface for $ArCl_2$ using the Møller−Plesset perturbation theory to second order (MP-2) and found general agreement of the calculated bond energy and bond length with experimental data. Calculations at the MP-4 level of theory for $ArCl_2$ were done by Sadlej *et al.*[21] Intramolecular vibrational redistribution in $ArCl_2$ was examined by Halberstadt *et al.*[22] using converged three-dimensional quantum mechanical calculations. Naumkin and Knowles[23] investigated the effect of anisotropy on interactions between atoms and applied their findings to the Ar−halogen systems. Finally McCourt *et al.*[24] employed an empirical potential energy surface and calculated several properties of $ArCl_2$ and compared them to experimental data.

This paper presents differential cross section (DCS) measurements for the Ne + Cl_2 and Ar + Cl_2 systems. The aim of this work is to determine potential energy surfaces for $HeCl_2$, $NeCl_2$, and $ArCl_2$ consistent with the available experimental data, including optical and microwave spectra as well as scattering distributions. For each molecule *ab initio* potentials were used as a starting point in a fit to these measured data. The fit to the data was performed in such a way that the fitted surface preserved, as much as possible, the anisotropy of the *ab initio* calculations. The fitted surfaces turned out to be not very different from the *ab initio* surfaces: the main difference is that *ab initio* calculations underestimate the depth of the potential wells.

This paper is organized as follows: section II contains information on the differential cross section measurements performed with a high-resolution crossed molecular beam apparatus in Perugia. Details on the potential function, DCS calculations, and fitting procedures are presented in section III. The results for $HeCl_2$, $NeCl_2$, and $ArCl_2$ are given in section IV and discussed in section V. Section VI concludes the paper with a brief summary and suggestions for future work.

II. Experimental Methods

Total (elastic and inelastic) differential cross sections for Ne−Cl_2 and Ar−Cl_2 were measured in Perugia using a high-resolution crossed molecular beam apparatus that has been described in detail elsewhere.[25] Briefly, well-collimated differentially pumped, supersonic nozzle beams of Ne (Ar) and Cl_2 are crossed at 90° in a large scattering chamber kept at 10^{-7} mbar, and the in-plane scattered rare gas atoms are detected by a rotating ultrahigh-vacuum quadrupole mass spectrometer detector. The most relevant data concerning the interacting beams are listed in Table 1. By using room temperature nozzles the resulting collision energies were $E = 70.7$ meV for Ne−Cl_2 and $E = 74.9$ meV for Ar−Cl_2. The Cl_2 pressure was kept low to avoid condensation. Test measurements carried out at different Cl_2 pressures showed no noticeable effect on the amplitude and location of the high-frequency oscillatory structure observed in the total DCS for Ne−Cl_2. The Cl_2 beam conditions were the same as used in previous experiments on the He−Cl_2 system, and the geometrical arrangement is the same as that used in previous experiments. The beam velocities have been measured by absolute time-of-flight analysis to within 1%, and the location of the primary beam was determined to within 0.03° as in previous work.[4] From the velocity distribution of the Cl_2 beam, a translational temperature of about 20 K is estimated. Assuming equilibrium between translational and rotational degrees of freedom, rotational states up to $j = 14$ (1%) are populated with a maximum at $j = 4-5$. The laboratory total angular distributions $I(\Theta)$ were obtained by taking from four to six scans and counting for 30−90 s at each angle, depending on signal intensity. The Cl_2 target beam was modulated at 160 Hz by a tuning fork chopper for background subtraction.

III. Computational Methods

A. Potential Form and DCS Calculations. MP-4 potential energy surfaces for the X states of the $RgCl_2$ systems[8] were used to calculate the differential cross sections of the Rg (rare gas) + Cl_2 collisions. The infinite order sudden approximation (IOSA)[26] was employed to perform these calculations. Pack[27] has clearly shown that damping of the rainbow and diffraction oscillations in the total DCS is directly related to the anisotropy of the depth (ϵ) and position (R_m), respectively, of the minimum of the potential well. It has been demonstrated for He−O_2 (ref 25), He−N_2 (ref 28), and He−CO_2 (ref 29) scattering that an evaluation of the quenching and shifting of the diffraction structure within the IOS approximation allows a reasonably accurate determination of the potential anisotropy, which (although obtained indirectly) is in agreement with that obtained directly from rotationally inelastic scattering data. Furthermore, an accurate (to within 1%) determination of the absolute distance scale of the potential can also be obtained from the locations

of the diffraction extrema. It thus seems reasonable to assume that this procedure, which has been used successfully for the determination of the O_2-, N_2-rare gas interactions,[25,28,30] can also be employed for the determination of the Cl_2-rare gas interactions. However, the wisdom of employing the IOSA for the calculation of the total DCS for the scattering of such relatively heavy collision partners, especially $Ar-Cl_2$, at collision energies as low as 70 meV might well be questioned. Direct comparison between exact close-coupling (CC) and IOSA computations for collisions involving He and Ne has firmly established[28,31,32,33] that the IOSA provides an accurate calculation of the total DCS at such collision energies. Indeed the IOSA was found to be inadequate only for large Δj transitions, which contribute little to the small angle total DCS.[28,32] Close-coupling calculations for $Ar-O_2$ at $E = 97$ meV (ref 34) indicate that the inelastic cross sections calculated within the IOSA disagree with those calculated using the close-coupling method only for rotational transitions that involve large values of Δj. These transitions were shown to contribute little to the total DCS up to laboratory angles of about 30°. It was concluded that it is reasonable to use the IOSA to fit total DCS data for systems such as $Ar-O_2$. Although the restrictions of validity of IOSA may be more severe in the case of $Ar-Cl_2$ because of the heavier mass and larger anisotropy, we have applied the IOSA for the analysis of the present scattering data. It must be noted that the primary reason for using the IOSA is that close-coupling computations of the total DCS for these systems involving a heavy molecule such as Cl_2, at the energy of the present experiments, are prohibitive.

The 1-center MSV potential form given in eqs 1−5 (and also employed by Huang *et al.*[5]) was fitted to the *ab initio* MP-4 points:

$$V(R,\gamma) = \epsilon(\gamma)\cdot f(x), \quad x = R/R_m(\gamma) \tag{1}$$

with the Legendre-expansions

$$\epsilon(\gamma) = \bar{\epsilon}\cdot[1 + A_2\cdot P_2(\cos(\gamma)) + A_4\cdot P_4(\cos(\gamma)) + A_6\cdot P_6(\cos(\gamma)) + A_8\cdot P_8(\cos(\gamma))] \tag{2}$$

and

$$R_m(\gamma) = \bar{R}_m\cdot[1 + B_2\cdot P_2(\cos(\gamma)) + B_4\cdot P_4(\cos(\gamma)) + B_6\cdot P_6(\cos(\gamma)) + B_8\cdot P_8(\cos(\gamma))] \tag{3}$$

R is the distance between the rare gas atom and the center of mass of Cl_2; γ is the angle between R and the Cl_2 molecular axis. The short-range and long-range parts of the potential are joined with the following Morse-spline-van der Waals (MSV) reduced form:

$$f(x) = \exp[-2\beta(x-1)] - 2\cdot\exp[-\beta(x-1)], \quad 0 < x < x_1$$

$$= b_1 + (x - x_1)\cdot\{b_2 + (x - x_2)\cdot[b_3 + (x - x_1)\cdot b_4]\}, \quad x_1 \le x \le x_2 \tag{4}$$

$$= -c_6\cdot x^{-6} - c_8\cdot x^{-8} - c_{10}\cdot x^{-10}, \; x_2 < x < \infty$$

with

$$\beta = \bar{\beta}\cdot(1 + \beta_2\cdot P_2(\cos(\gamma))),$$

$$c_6 = \frac{\bar{C}_6}{\bar{\epsilon}\cdot\bar{R}_m^6}, \quad c_8 = \frac{\bar{C}_8}{\bar{\epsilon}\cdot\bar{R}_m^8}, \quad c_{10} = \frac{\bar{C}_{10}}{\bar{\epsilon}\cdot\bar{R}_m^{10}} \tag{5}$$

The $\bar{C}_6$, $\bar{C}_8$, and $\bar{C}_{10}$ constants were derived following the procedure outlined in ref 4. The resulting analytical potential was used to calculate the differential scattering cross sections within the IOSA. The approximation involves a 32-point Gauss-Legendre quadrature, which was used to average the center-of-mass (c.m.) cross sections $\sigma(\Theta,\gamma)$ over $\cos(\gamma)$, according to the IOSA formula

$$\sigma(\Theta) = \frac{1}{2}\cdot\int_{-1}^{+1}\sigma(\Theta,\gamma)\, d[\cos(\gamma)] \tag{6}$$

To compare the calculated cross sections with the experimental angular distributions $I(\Theta)$, a transformation from the c.m. system into the laboratory frame was performed by using the elastic Jacobian. The result was then averaged over the velocity distributions of the two beams and over the beam/detector geometry, as done in previous work.[4,35]

B. Fits of the Potential Energy Surfaces to Experimental Data. For all three $Rg-Cl_2$ molecules, the *ab initio* potential energy surfaces[8] yielded a scattering distribution that showed substantial differences compared to the measured distributions, see section IV. However, the results were promising enough that the *ab initio* surfaces were taken as the starting points for a fit to the data, and the fit was performed in such a way as to preserve the anisotropy of the *ab initio* surface. Three types of experimental data were employed: the measured differential cross sections $I_{exp}(\Theta)$ for the $Rg + Cl_2$ collisions, the experimental dissociation energies for the $NeCl_2 \rightarrow Ne + Cl_2$ and $ArCl_2 \rightarrow Ar + Cl_2$ processes,[15,36,37] and the three asymmetric rotor rotational constants A, B, and C.[38] The fit was performed with a versatile genetic algorithm (GA) driver,[39] available as freeware on the World Wide Web. The calculations were done on DEC Alpha workstations. The GA decides on a new set of potential parameters, which are used to calculate the DCS, dissociation energy, and three rotational constants. For $NeCl_2$ and $ArCl_2$ three least-squares values, χ_i^2 ($i = 1, ..., 3$), were calculated and weighted according to the following formula:

$$c_{fitness} = \frac{1}{[(\chi_1^2)^x\cdot(\chi_2^2)^y\cdot(\chi_3^2)^z]} \tag{7}$$

The exponents x, y, and z in eq 7 were chosen as follows: the weighting of the spectroscopy was kept as low as possible but high enough to yield rotational constants within the experimental error bars. Similarly, the weighting of the scattering data was choosen to be as low as possible but still sufficiently high to reproduce the experimental DCS. For the $NeCl_2$ fit the exponents were $x = 4$, $y = 2$, and $z = 0.5$. For $ArCl_2$, $x = 3$, $y = 1$, and $z = 0.5$. The χ_i^2 values were calculated according to the following equations:

$$\chi_1^2 = (1_{01} - (B + C))^2 + (1_{11} - (A + C))^2 + (1_{01} - (A + B))^2 \tag{8}$$

$$\chi_2^2 = \sum_{\Theta}(I_{calc}(\Theta) - I_{exp}(\Theta))^2 \tag{9}$$

and

$$\chi_3^2 = (D_0^{calc} - D_0^{exp})^2 \tag{10}$$

In eqs 8−10, 1_{01}, 1_{11}, and 1_{10} represent the lowest three calculated rotational energies for $J = 1$; $I_{calc}(\Theta)$ and D_0^{calc} are the calculated scattering distributions and dissociation energies, respectively. The fitness value $c_{fitness}$ for $HeCl_2$ was $1/(\chi_1^2\cdot(\chi_2^2)^2)$ (an experimental value for the $HeCl_2$ dissociation energy does not exist). The GA driver works to *maximize* the value $c_{fitness}$ by varying the potential parameters, within the limits specified by the user, in such a way to efficiently sample the

TABLE 2: Results of the Calculations with the *ab Initio* And Best Fit Potential Energy surfaces

	rotational constants (cm^{-1})			diss. energy D_0 (cm^{-1})			Rg−Cl_2 distance R_0[a] (Å)		
	measured	*ab initio*	best fit	measured	*ab initio*	best fit	measured	*ab initio*	best fit
$HeCl_2$	$A = 0.31(5)$ $B = 0.2435$ $C = 0.14(1)$	$A = 0.313$ $B = 0.275$ $C = 0.126$	$A = 0.304$ $B = 0.256$ $C = 0.131$		12.20	18.43	3.8 ± 0.4	4.0 ± 0.3	3.9 ± 0.1
$NeCl_2$	$A = 0.2435$ $B = 0.085(2)$ $C = 0.063(1)$	$A = 0.2485$ $B = 0.0830$ $C = 0.0612$	$A = 0.2484$ $B = 0.0853$ $C = 0.0625$	59.7 ± 2.0	56.0	61.5	3.57 ± 0.04	3.63 ± 0.02	3.58 ± 0.02
$ArCl_2$	$A = 0.245\ 953(4)$ $B = 0.048\ 169\ 591(8)$ $C = 0.040\ 0381\ 28(7)$	$A = 0.244\ 74$ $B = 0.045\ 59$ $C = 0.038\ 24$	$A = 0.24596$ $B = 0.048\ 16$ $C = 0.040\ 05$	187.9 ± 1.0	178.45	188.40	3.7190 ± 10^{-6}	3.818 ± 0.006	3.715 ± 0.006

[a]The error bars for the *ab initio* and best fit R_0 reflect the uncertainties in using the rigid-rotor approximation and not errors in the potential energy surface.

"parameter space". This efficiency is quite important in this study, because each calculation of the "data" from subsequent iterations of the potential is quite time consuming.

In the case of $HeCl_2$ the leading terms ($\bar{\epsilon}$ and $\bar{R}_m$) and first anisotropy parameters (A_2 and B_2) were varied, and all other potential parameters were held fixed to the *ab initio* values. For $NeCl_2$ only the leading terms of well depth ($\bar{\epsilon}$), equilibrium distance ($\bar{R}_m$), and steepness ($\bar{\beta}$) were allowed to vary, and all the anisotropy parameters were held fixed at the values obtained from the *ab initio* calculations. In the case of $ArCl_2$ all the leading terms ($\bar{\epsilon}$, $\bar{R}_m$, and $\bar{\beta}$) and the first anisotropy parameters (A_2 and B_2) were varied while the others were held at the *ab initio* values, but the potential parameters from an MP-4 *ab initio* surface, adjusted with CCSD(T) (coupled cluster approach with singles, doubles, and noniterative triples) points,[8] were used as starting values in the fit.

To determine the sensitivity of the potential to the region of the potential near the linear configuration, all-parameter fits with potential energy surfaces that had fixed linear well depths were carried out. Linear well depths ±10% (±20% for $ArCl_2$) of the best fit values were tested. Since the spectroscopic data is most sensitive to the perpendicular region, this data could be reproduced with these restricted surfaces. However, the scattering data are also sensitive to the linear well region, and we conclude that the linear well depths are accurate to ±10% (±20% for $ArCl_2$). We chose to test the sensitivity to the linear well depths in this way because the GA does not give error bars for the parameters. Even if a more standard routine, such as the Marquardt nonlinear algorithm, were employed, the correlation matrix for the parameters would not be particularly useful for this problem. The highly anisotropic potential that must be employed to fit the *ab initio* points has far more parameters than can be determined from available data. It is also not obvious how to incorporate the *ab initio* points directly into the fit since there are systematic errors in these points. For instance, the calculated well depths are clearly too shallow. For these reasons we incorporated the methods described above, which rely on our physical insight in choosing which parameters to float.

There are other technical issues that need to be mentioned in choosing a fitting strategy. For each test potential considerable computer power is expended to calculate "data" for comparison to the experiment. For the rotational constants and dissociation energy, a full J dependent variational calculation of the bound state energies (similar to those described in refs 4 and 5) must be performed. Since the cost, in time, of these calculations increases rapidly with basis set size, compromises must be made. This keeps us from taking full advantage of the many significant figures of the microwave data for $ArCl_2$. Similarly, the infinite order sudden (IOS) approximation used to calculate the DCS distributions cannot be completely tested. It is expected to be quite good for small angles but to degrade for larger angles due to increased inelasticity, especially for $ArCl_2$. In preliminary test calculations by D. Lemoine,[40] the scattering intensity calculated for low-energy helium scattering using the close-coupling method shows the IOSA approximation to be valid up to 16°; at the higher energy, IOSA is expected to be valid in all the experimental angular range. Another assumption that can affect the large angle scattering intensities is the use of the elastic Jacobian. A more extensive test of the potentials reported here by higher level calculations would be very valuable but is beyond the scope of this paper. At the present time, close-coupling calculations for Ar−Cl_2 are prohibitively time consuming.

IV. Results

Table 2 gives an overview over the results obtained by calculations with the *ab initio* surfaces of $HeCl_2$, $NeCl_2$, and $ArCl_2$, as well as the results from fitting the surfaces to the experimental data. The values for R_0 (Rg−center-of-mass Cl_2 distance) in Table 2 were calculated from the rotational constants using a rigid rotor model. Since Rg−Cl_2 molecules are not rigid rotors, the two rotational constants depending on R_0 (A and C for $HeCl_2$, B and C for $NeCl_2$, $ArCl_2$) give two different distances. Therefore a range of R_0 is reported in Table 2. Contour plots of the best fit surfaces are shown in Figure 1.

A. $HeCl_2$. Figure 2 shows the calculated differential cross section obtained with the *ab initio* potential for $HeCl_2$ together with the experimental data. Here the collision energy is $E =$ 68.8 meV. The laboratory angular distributions are also reported multiplied by $\Theta^{7/3}$ in order to remove the steep angular dependence at small angles and to enhance the oscillatory structure. Only the remainder of the main rainbow oscillation is discernible as the first maximum at about 4°. It can be seen that the locations of the maxima and minima of the diffraction oscillations in the calculated DCS do not match very well with the ones in the measured data. Also at higher angles the DCS intensities do not agree very well, which is probably due to the IOS approximation. Both the location of the calculated rainbow maximum (at too small of an angle) and the shift of the calculated diffractions (toward too small angles) with respect to experiment suggest that the well depth should be deeper and the minimum position closer. Also, the diffraction amplitudes are predicted to be somewhat too quenched, which indicates that the anisotropy parameters should be smaller. Indeed, by allowing the parameters $\bar{\epsilon}$, A_2, $\bar{R}_m$, and B_2 to vary, one obtains a much better fit to the experimental data, see Figure 3. The value χ_2^2 for this fit was 0.0024, which should be compared to the value 0.031 for the fit in Figure 3 of ref 5 (SA-MSV fit). For a lower collision energy, $E = 24.7$ meV, the experimental DCS and the calculated curve obtained using the best fit PES are shown in Figure 4. Again we obtain a better fit with $\chi_2^2 =$

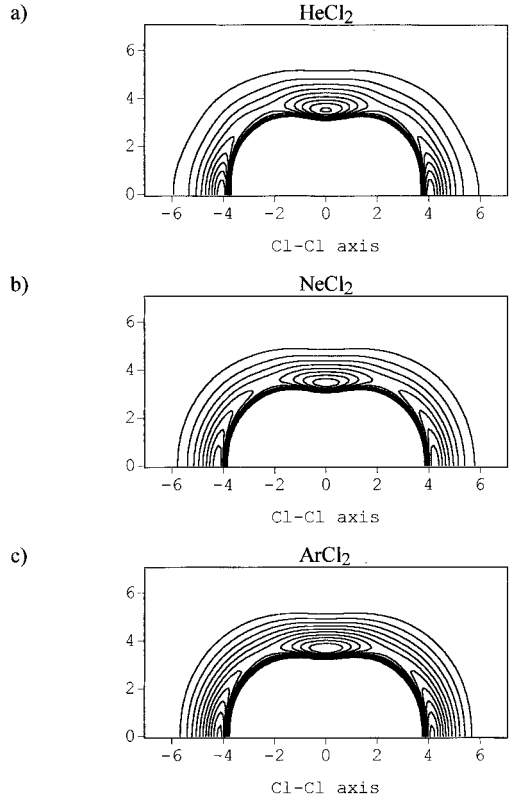

Figure 1. Best fit potential energy surfaces of the $HeCl_2$ (a), $NeCl_2$ (b), and $ArCl_2$ (c) molecules in the X electronic state. The Cl atoms are located at ±0.995 Å on the horizontal axis of the plot. The units are Å on both axes, and the energies are relative to the rare gas−Cl_2 dissociation limit. (a) For $HeCl_2$, contours have a spacing of 5 cm^{-1} and the outermost is at −5 cm^{-1}. The T-shaped well is at R = 3.524 Å and has an energy of −45.98 cm^{-1}. The linear well is at R = 4.051 Å and has an energy of −49.34 cm^{-1}. The saddle point is located at 55.7° and R = 4.245 Å with an energy of −21.14 cm^{-1}. (b) For $NeCl_2$, contours have a spacing of 10 cm^{-1} and the outermost is at −10 cm^{-1}. The T-shaped well is at R = 3.445 Å and has an energy of −86.94 cm^{-1}. The linear well is at R = 4.213 Å and has an energy of −87.13 cm^{-1}. The saddle point is located at 56.2° and R = 4.125 Å with an energy of −47.18 cm^{-1}. (c) For $ArCl_2$, contours have a spacing of 20 cm^{-1} and the outermost is at −20 cm^{-1}. The T-shaped well is at R = 3.657 Å and has an energy of −220.83 cm^{-1}. The linear well is at R = 4.132 Å and has an energy of −226.88 cm^{-1}. The saddle point is located at 54.3° and R = 4.244 Å with an energy of −127.36 cm^{-1}.

0.0065, compared to a value of 0.067 in Figure 3 of ref 5. Note that the low-energy data was not used in the fit, so the agreement of the calculated DCS with the experimental data is a test of the reliability of the fit. Note in particular the quality of the present fit of the third maximum at about 18°, which was not very well reproduced in the SA-MSV fit.[5]

A contour plot of the best fit potential energy surface is shown in Figure 1, and the potential parameters are given in Table 3. Cuts through the unchanged *ab initio* and fitted potentials at 0°, 90° and the saddle point are depicted in Figure 5. The linear and T-shaped wells of the fitted surface are both deeper than the corresponding wells of the *ab initio* surface. Table 3 gives more details on the features of both surfaces. The fitted surface gives a dissociation energy D_0 of 18.43 cm^{-1}, and the calculated He−Cl_2 distance R_0 is 3.9 Å, which is consistent with the LIF-measurements[3] (R_0 = 3.8 ± 0.4 Å). The calculated rotational constants are A = 0.304 cm^{-1}, B = 0.256 cm^{-1} and C = 0.131 cm^{-1}. A is off by 2%, B is off by 5%, and C is off by 6% compared to experimental results.[38] The errors of the rotational constants are rather large, because we fitted to rigid-rotor values. For the X state of $HeCl_2$ a rigid-rotor model works only reasonably well, see ref 9. However, the rigid-rotor rotational constants provide the most useful constraints for the fitting. A

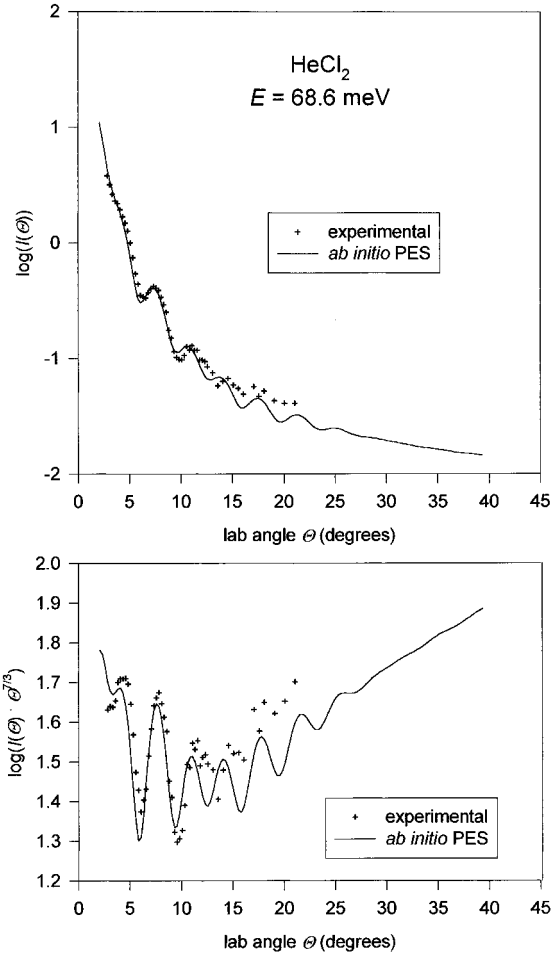

Figure 2. Total differential cross sections for the scattering of He from Cl_2 with a collision energy of 68.8 meV. Crosses are the measured values, and the solid line was calculated using the MP-4 *ab initio* surface for $HeCl_2$ and the IOS approximation.

TABLE 3: Potential Parameters for the *ab Initio* and Best Fit × Electronic State 1-Center MSV PES of $HeCl_2$. The Cl−Cl Distance r Was 1.990 Å

parameter	*ab initio*	best fit
$\bar{\epsilon}$/cm^{-1}	24.2870	30.1862
A_2	−0.16976	−0.2000
A_4	0.7608	0.7608
A_6	−0.2022	−0.2022
A_8	0.2772	0.2772
$\bar{R}_m$/Å	4.034	4.0318
B_2	0.1611	0.1255
B_4	−0.1345	−0.1345
B_6	0.02814	0.02814
B_8	−0.0144	−0.0144
$\bar{\beta}$	6.3741	6.3741
β_2	0.250	0.250
x_1	1.108744	1.108744
x_2	1.50	1.50
$\bar{C}_6$/cm^{-1} Å^6	107000	107000
$\bar{C}_8$/cm^{-1} Å^8	724000	724000
$\bar{C}_{10}$/cm^{-1} Å^{10}	6477000	6477000
well depth (cm^{-1}) (γ = 0°)	−40.44	−49.34
well depth (cm^{-1}) (γ = 90°)	−36.63	−45.98
well position (Å) (γ = 0°)	4.197	4.051
well position (Å) (γ = 90°)	3.454	3.524

direct calculation of the transition energies would require an new set of assumptions for the excited state surface.

B. $NeCl_2$. For $NeCl_2$ the experimental data (Figure 6) clearly exhibit the main rainbow structure with superimposed diffraction oscillations. The scattering distribution calculated from the *ab initio* surface (Figure 6) showed diffraction maxima and minima that were out of phase with respect to the experimental data,

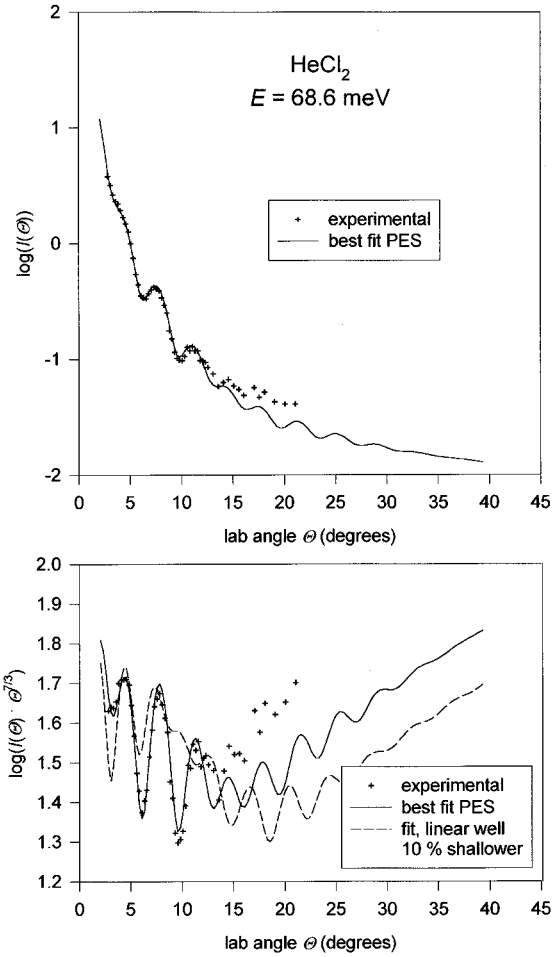

Figure 3. Total differential cross sections for the scattering of He from Cl_2 with a collision energy of 68.8 meV. Crosses are the measured values, and the solid line was calculated using the best fit surface for $HeCl_2$ and the IOS approximation. The dashed line represents the result obtained with a 10% shallower linear well depth.

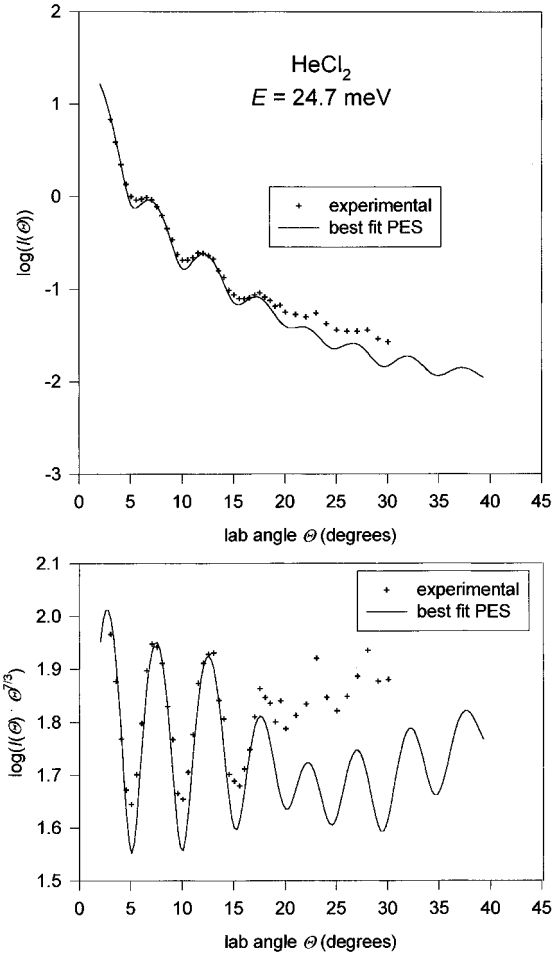

Figure 4. Total differential cross sections for the scattering of He from Cl_2 with a collision energy of 24.7 meV. Crosses are the measured values, and the solid line was calculated using the best fit surface for $HeCl_2$ and the IOS approximation.

TABLE 4: Potential Parameters for the *ab Initio* and Best Fit × Electronic State 1-Center MSV PES of $NeCl_2$. The Cl−Cl Distance *r* Was 1.990 Å

parameter	*ab initio*	best fit
$\bar{\epsilon}$/cm^{-1}	58.5791	63.0376
A_2	−0.1056	−0.1056
A_4	0.5683	0.5683
A_6	−0.2320	−0.2320
A_8	0.1525	0.1525
$\bar{R}_m$/Å	4.0107	3.9627
B_2	0.1542	0.1542
B_4	−0.1086	−0.1086
B_6	0.0303	0.0303
B_8	−0.0126	−0.0126
$\bar{\beta}$	6.8089	6.5557
β_2	0.1945	0.1945
x_1	1.101800	1.101800
x_2	1.50	1.50
$\bar{C}_6$/cm^{-1} Å^6	236000	236000
$\bar{C}_8$/cm^{-1} Å^8	1710000	1710000
$\bar{C}_{10}$/cm^{-1} Å^{10}	16570000	16570000
well depth (cm^{-1}) ($\gamma = 0°$)	−79.68	−87.13
well depth (cm^{-1}) ($\gamma = 90°$)	−79.50	−86.94
well position (Å) ($\gamma = 0°$)	4.265	4.213
well position (Å) ($\gamma = 90°$)	3.486	3.445

and the rainbow maximum is shifted toward small angles. Again, these deviations indicate that the well should be deeper. Figure 7 shows the best fit calculated scattering cross section distribution for $NeCl_2$. As can be seen, the calculated scattering distribution follows the measured distribution very closely: even details like the rapid oscillations are well reproduced. The fitted

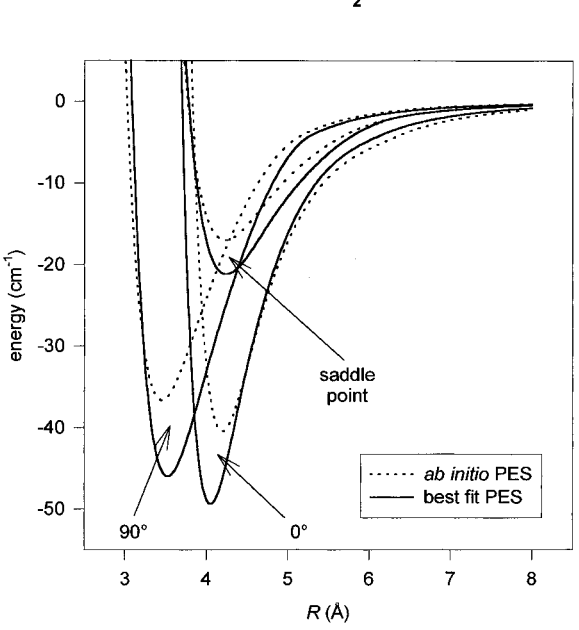

Figure 5. Cuts though the best fit and *ab initio* potential energy surfaces for $HeCl_2$ at $\gamma = 0°$, $\gamma = 90°$, and the saddle point.

$NeCl_2$ potential parameters are given in Table 4, and a contour plot of this surface is shown in Figure 1. Figure 8 shows cuts through the *ab initio* and fitted potential surfaces at 0°, 90°, and the saddle point. This potential energy surface gave a dissociation energy of $D_0 = 61.5$ cm^{-1}, within experimental

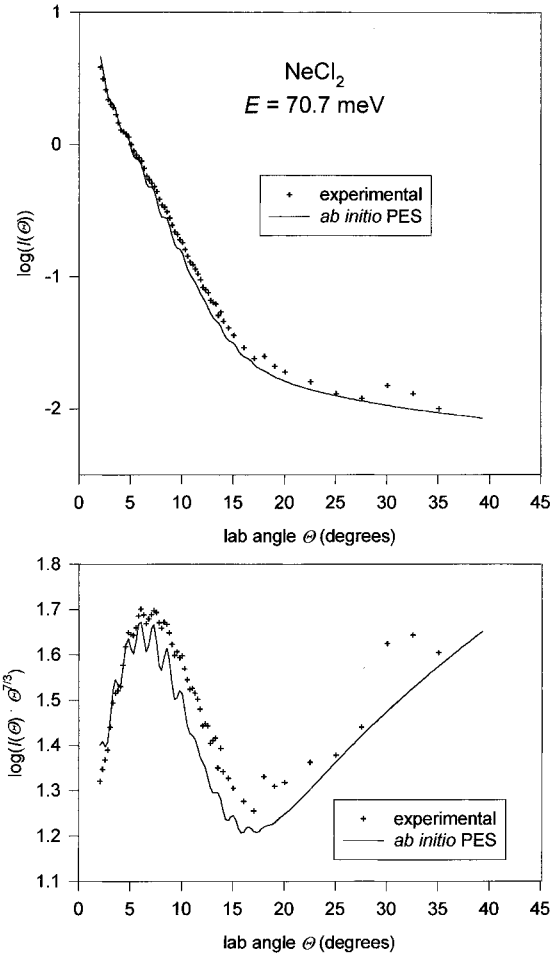

Figure 6. Total differential cross sections for the scattering of Ne from Cl_2 with a collision energy of 70.7 meV. Crosses are the measured values, and the solid line was calculated using the MP-4 *ab initio* surface for $NeCl_2$ and the IOS approximation.

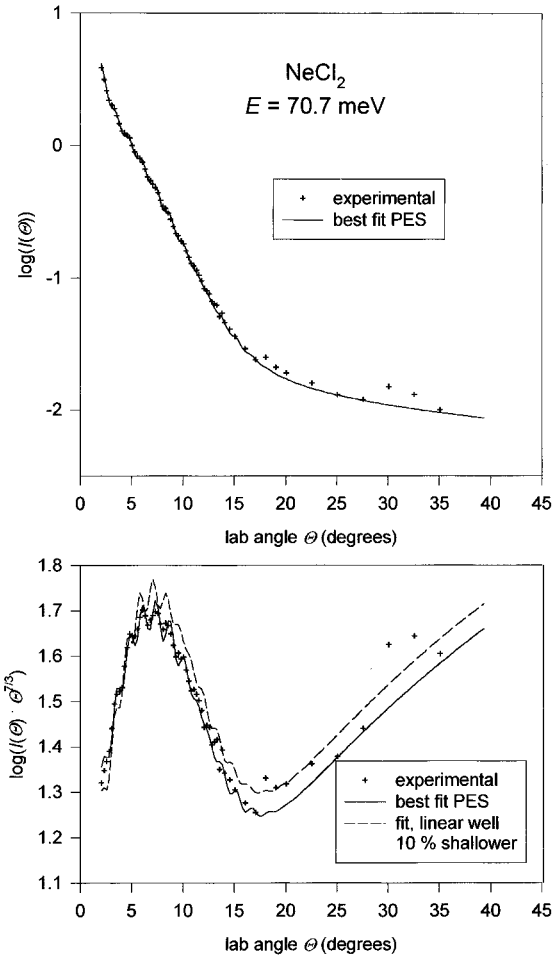

Figure 7. Total differential cross sections for the scattering of Ne from Cl_2 with a collision energy of 70.7 meV. Crosses are the measured values, and the solid line was calculated using the best fit surface for $NeCl_2$ and the IOS approximation. The dashed line represents the result obtained with a 10% shallower linear well depth.

error of the measured value (59.7 ± 2.0 cm^{-1}). The calculated Ne-Cl_2 distance R_0 is 3.58 Å, consistent with the value obtained from LIF measurements ($R_0 = 3.57 \pm 0.04$ Å). The calculated rotational constants are $A = 0.2484$ cm^{-1}, $B = 0.0853$ cm^{-1}, and $C = 0.0625$ cm^{-1}. These values are within or very close to the experimental error bars. (The constant A does not depend on the Ne$-$$Cl_2$ potential within the rigid-rotor approximation.) The major difference between the fitted surface and the one obtained from *ab initio* calculations is a 9% increase in the depth of both the linear and T-shaped well. Again, the *ab initio* calculations underestimate the well depth of the potential.

C. $ArCl_2$. Figure 9 shows the DCS data for Ar + Cl_2 compared to that calculated from the *ab initio* potential energy surface. For this system, which is characterized by a stronger van der Waals interaction, the data exhibit only the main rainbow and two supernumerary rainbow oscillations. For this heavier system the diffractions are too closely spaced to be resolvable under the present experimental conditions. Both the diffraction and the rainbow oscillations are dramatically quenched with respect to what one would measure if the interaction were spherical. The quenching effect is a manifestation of the anisotropy of the potential energy surface governing the scattering dynamics. The comparison between the calculated and the experimental data is less than satisfactory: the rainbow maxima and minima are dephased with respect to the experimental curve. The fact that the calculated rainbow maximum is significantly shifted toward small angles with respect to experiment indicates that the *ab initio* well depth is again considerably too shallow. The scattering distribution calculated with the best-fit potential is shown in Figure 10. The angular

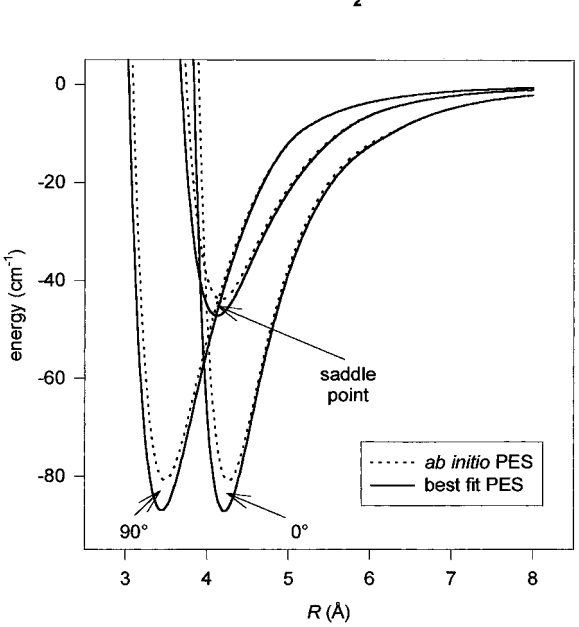

Figure 8. Cuts though the best fit and *ab initio* potential energy surfaces for $NeCl_2$ at $\gamma = 0°$, $\gamma = 90°$, and the saddle point.

positions of the maxima and minima are reproduced correctly, but at greater scattering angles there is an underestimation of the measured intensities. This is most likely due to the inadequacy of the IOS approximation at large scattering angles,

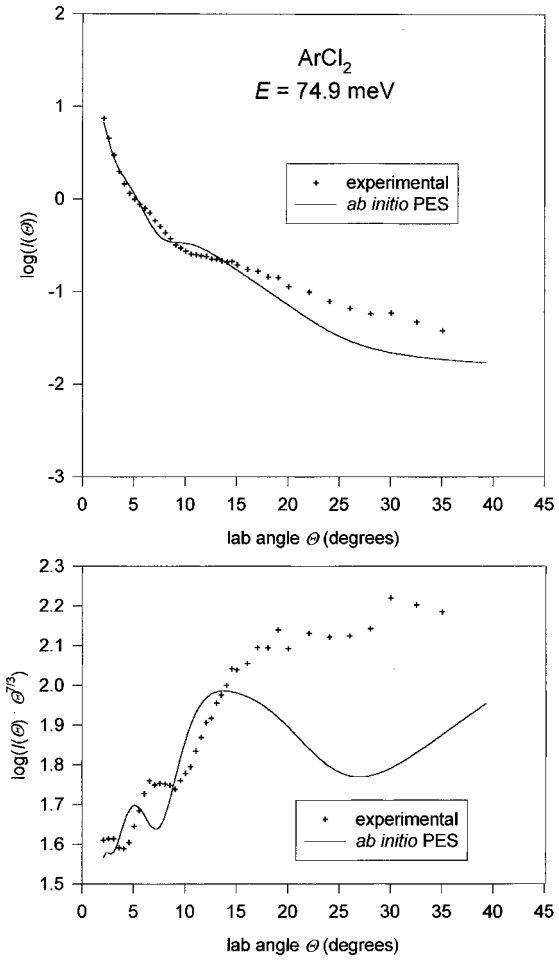

Figure 9. Total differential cross sections for the scattering of Ar from Cl_2 with a collision energy of 74.9 meV. Crosses are the measured values, and the solid line was calculated using the CCSD(T) corrected MP-4 *ab initio* surface for $ArCl_2$ and the IOS approximation.

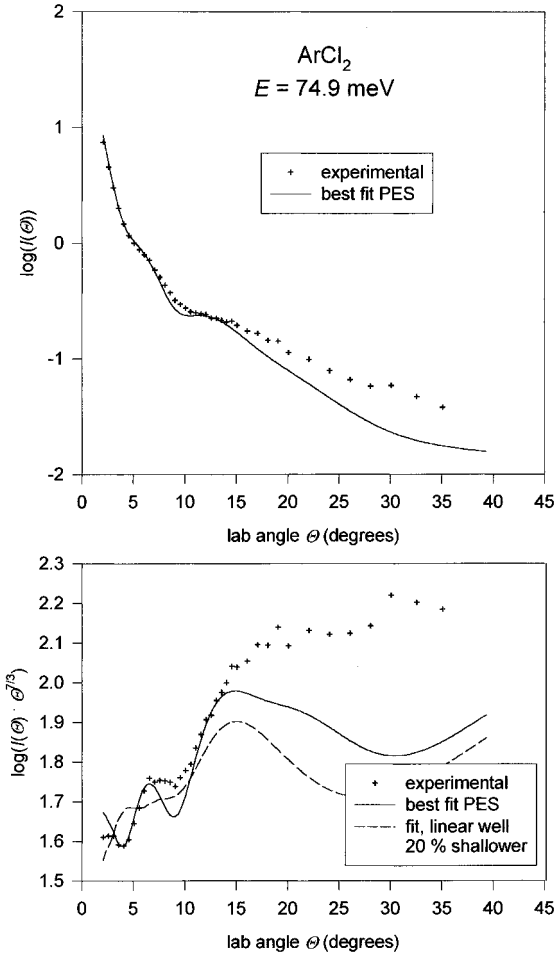

Figure 10. Total differential cross sections for the scattering of Ar from Cl_2 with a collision energy of 74.9 meV. Crosses are the measured values, and the solid line was calculated using the best fit surface for $ArCl_2$ and the IOS approximation. The dashed line represents the result obtained with a 20% shallower linear well depth.

TABLE 5: Potential Parameters for the *ab Initio* and Best Fit × Electronic State 1-Center MSV PES of $ArCl_2$. The Cl−Cl Distance *r* Was 1.990 Å

parameter	*ab initio*	best fit
$\bar{\epsilon}$/cm^{-1}	156.4612	164.1150
A_2	−0.1225	−0.1208
A_4	0.5339	0.5339
A_6	−0.1604	−0.1604
A_8	0.1307	0.1307
$\bar{R}_m$/Å	4.2509	4.0658
B_2	0.1399	0.1026
B_4	−0.1000	−0.1000
B_6	0.0263	0.0263
B_8	−0.0126	−0.0126
$\bar{\beta}$	6.4831	6.334
β_2	0.1758	0.1758
x_1	1.106916	1.106916
x_2	1.50	1.50
$\bar{C}_6$/cm^{-1} Å^6	826000	826000
$\bar{C}_8$/cm^{-1} Å^8	7020000	7020000
$\bar{C}_{10}$/cm^{-1} Å^{10}	77580000	77580000
well depth (cm^{-1}) ($\gamma = 0°$)	−216.03	−226.88
well depth (cm^{-1}) ($\gamma = 90°$)	−210.66	−220.83
well position (Å) ($\gamma = 0°$)	4.479	4.132
well position (Å) ($\gamma = 90°$)	3.745	3.657

where the contribution of inelasticity is larger. The potential parameters for the fitted surface are summarized in Table 5, and a contour plot of the potential energy surface is shown in Figure 1. Figure 11 shows cuts through the unchanged *ab initio* and fitted potential energy surfaces at 0°, 90°, and the saddle point. The T-shaped and linear wells of the fitted potential energy surface are about 5% deeper than the corresponding wells

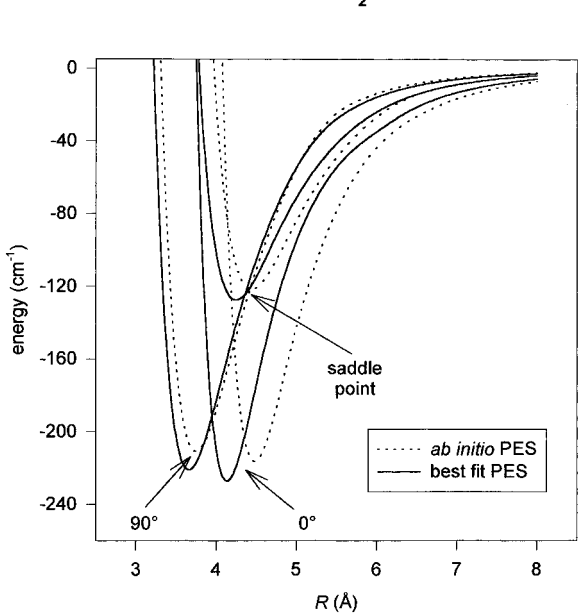

Figure 11. Cuts through the best fit and *ab initio* potential energy surfaces for $ArCl_2$ at $\gamma = 0°$, $\gamma = 90°$, and the saddle point.

of the *ab initio* surface. The calculated dissociation energy is $D_0 = 188.4$ cm^{-1} (187.9 ± 1.0 cm^{-1} is the experimental value[36]). The calculation gives $R_0 = 3.715$ Å, and the microwave data[19] gives $R_0 = 3.7190$ Å. The calculated

rotational constants are $A = 0.24596\ cm^{-1}$, $B = 0.04816\ cm^{-1}$, and $C = 0.04005\ cm^{-1}$. A is off by 0.003%, B by 0.02%, and C by 0.03% compared to the microwave values.[38] The microwave spectra result in extremely accurate values for the rotational constants, which we have only reproduced to ~0.02% accuracy. In principle, it would not be difficult to achieve a better fit. However, two practical problems have kept us from taking this next step. First, if we were to float more of the anisotropy parameters, there is no longer a unique fit, and the automated search yields a physically unreasonable anisotropy. Second, the variational calculation of the rotational constants from the potential energy surface would require a much larger basis to achieve microwave accuracy, and the necessary convergence criteria would require considerable extra computer time.

V. Discussion

It is obvious that to obtain the best potential energy surface for any particular interaction, as much information as possible should be incorporated into the fit. In particular, *ab initio* calculations for interactions such as those of the noble gas−halogens are now accurate enough that such information must be included in the fit. However, the best way to include different types of information is not so obvious. The *ab initio* calculations clearly show that relatively simple potential forms, such as those of refs 4 and 24, are not nearly anisotropic enough to be realistic. However, we have not been able to define a potential function that can be adjusted to be more consistent with the *ab initio* points without adding more parameters than can be adequately determined by experimental data. For this reason we have implemented a hybrid approach in which the *ab initio* calculations provide the starting point of the fit, and physical intuition is employed to vary a few parameters to fit the experimental data while maintaining the essential aspects of the calculated anisotropy.

The results presented above show that the *ab initio* surfaces can be adjusted to fit experimental data with fairly minor modifications. For each of the three noble gases, the depth of the well had to be increased and the distance to the well minimum had to be slightly decreased. However, the essential aspects of the anisotropy, the deep linear well separated from the perpendicular well by a considerable barrier, is clearly consistent with the data in each case. That the deeper linear minimum is consistent with the experimental observation of a perpendicular ground state is due to zero-point energy effects as discussed previously.[5,8] Recently, Cockett *et al.*[41] found experimental evidence for both linear and perpendicular isomers of ArI_2. Also, Klemperer and colleagues[42] have shown that microwave and far-infrared spectra of HeClF are in near quantitative agreement with the anisotropy calculated at the MP-4 level with basis sets analogous to those employed in this study. In the case of HeClF the data is highly sensitive to both the He−Cl−F linear well and the perpendicular well. As in our study, Klemperer and colleagues can improve the quality of the fit to the data by increasing the average well depth. The cumulative evidence for the linear well is now very strong.

Interestingly, the extent to which the *ab initio* surfaces had to be changed to fit the data was different for He−, Ne−, and Ar−Cl_2. It is particularly interesting that the smallest adjustments were required for $NeCl_2$, even though that is the molecule for which the data provide the most stringent constraints. No spectroscopic dissociation energy is available for $HeCl_2$, and the DCS data for $NeCl_2$ is much more detailed than for $ArCl_2$. For $NeCl_2$ only the leading terms for the well depth, well distance, and steepness needed to be adjusted to fit the data. The fit of the $HeCl_2$ and $ArCl_2$ *ab initio* surfaces to the data required small adjustments of the first anisotropy parameters of well depth and well distance.

The DCS of $HeCl_2$, calculated with the *ab initio* surface (Figure 2), shows that the remainder of the main rainbow is predicted to be at slightly smaller angles compared to the measured curve, so according to

$$q \cong \frac{2\bar{\epsilon}}{E} \tag{11}$$

(see ref 43), the true well depth $\bar{\epsilon}$ should be larger. Indeed, $\bar{\epsilon}$ for the best fit surface is 24% larger than for the *ab initio* surface (Table 3). The same argument holds for $NeCl_2$, see Figures 6 and 7. The calculated rainbow position for the *ab initio* surface is shifted toward smaller angles. Again, the best fit $\bar{\epsilon}$ is larger by 8% than the one obtained from the MP-4 data (see Table 4). Also for $ArCl_2$ the rainbow angle calculated with the *ab initio* PES is too small. The fit corrects for this behavior by increasing the well depth by 5% (Table 5). The frequency of the diffraction oscillations are described[43] by

$$\Delta\theta = \frac{\pi \cdot \hbar}{\mu \cdot v \cdot \bar{R}_m} \tag{12}$$

The *ab initio* predictions for $HeCl_2$ and $NeCl_2$ show near agreement with the experimental features, so the fit does not change the $\bar{R}_m$ values very much. For $ArCl_2$ the diffraction oscillations are too closely spaced to be resolved in the measurements, so $\Delta\theta$ cannot be determined; however, the rainbow structure is not only sensitive to $\bar{\epsilon}$, but also to $\bar{R}_m$.[43]

It is also interesting to note that for $ArCl_2$ a CCSD(T)-modified MP-4 *ab initio* surface had to be used as starting point in the multiproperty fit. Attempts to use the unmodified MP-4 surface did not succeed. The CCSD(T) level of theory is able to predict the anisotropy of the PES, which was not changed in the fit. This level of theory was also found to be necessary in determining the *ab initio* geometry of the $ArCl_2$ molecule.[8]

The potentials of refs 4 and 24, which have a linear saddle instead of a linear minimum, could probably be adjusted to fit the DCS data with minor modifications. We have not, however, performed serious tests of these potentials because they are completely inconsistent with the *ab initio* points. Still, the ability of such potentials to nearly fit the data might cause one to infer that the data by itself cannot provide any useful constraints on the depth of the linear well. However, we showed above that if we added the constraint that the linear well depth is 10% less than the best fit value for $HeCl_2$ and $NeCl_2$, or 20% less for $ArCl_2$, then the quality of the fits obtained is considerably degraded. This is true even if we compensate for the extra constraint by floating all of the anisotropy parameters and dropping any preconceptions of how the surface should look. We do not completely understand the reason why both a deep linear well minimum and no minimum are consistent with the data, but a linear minimum with an intermediate well depth is not. It is clear that the constraints provided by experimental data lead to a complex least-squares topography in the parameter space of the potential functions that are used. This is, of course, the main difficulty in obtaining fitted potential surfaces. We are convinced that the observed sensitivity to the linear well depth is realistic and that new data or higher level calculations will not force qualitative changes onto the anisotropies that we employ in this study. We also note that the linear wells cannot be much deeper than those we obtain without causing the ground state of each molecule to switch to the linear minimum.

VI. Summary and Conclusions

Differential scattering cross sections for the He−Cl_2, Ne−Cl_2, and Ar−Cl_2 collisions were measured and analyzed together

with spectroscopic data on these systems. *Ab initio* potential energy surfaces were employed to calculate the experimental data, but it was found to be necessary to adjust the surfaces to obtain quantitative agreement with the measurements. Most importantly, the well depth had to be increased for each molecule. The *ab initio* surfaces for $HeCl_2$ and $ArCl_2$ had to be changed in the leading terms and first anisotropy parameters of well depth and minimum distance, while the anisotropy parameters were held fixed in the fit for $NeCl_2$. In all cases the essential aspects of the *ab initio* anisotropies were preserved in the fits. For each of the three molecules the linear well of the best fit surface is still slightly deeper than the perpendicular well. For $NeCl_2$, very slight adjustments of the *ab initio* data yielded excellent fits to the details of the experimental data. In this case the linear and perpendicular well depths are nearly equal. The fitted potentials are consistent with the experimental DCS within the infinite order sudden approximation, but the calculations for $HeCl_2$ and $ArCl_2$ show some discrepancies at higher angles. This disagreement at high angles may be due to the IOS approximation, as discussed earlier.

We believe that the best fit potential energy surfaces presented here for these molecules are the best surfaces that can be constructed using currently available information. Of course, the present work is not very sensitive to either the very short range or very long range portions of the potential. Also, the present data does not specify how the rare gas−Cl_2 potential depends on the Cl−Cl distance. For this important aspect of the potential, stimulated emission pumping data for high vibrational levels of the X state would be very useful. New data regarding either the linear isomers or excited vibrational levels would also be very valuable. Given the central role that rare gas−halogen species play in many dynamical studies, further work on this difficult problem is well justified.

Acknowledgment. L.B., P.C., and G.G.V. acknowledge financial support from the Italian "Consiglio Nazionale delle Ricerche, Progetto Finalizzato Chimica Fine" and "Ministero Universitá e Ricerca Scientifica". The work in Irvine was supported by the National Science Foundation and by the Air Force Office of Scientific Research. We thank the Office of Academic Computing at UCI for access to the Convex computer and the Institute of Surface and Interface Science for access to DEC Alpha workstations. A.R. would like to thank the Swiss National Science Foundation for a fellowship. The authors also thank David L. Carroll, University of Illinois at Urbana-Champaign, Urbana, for the FORTRAN GA driver. We are grateful to Nadine Halberstadt for letting us use her bound state program and to Jason Williams for setting up the GA program. We thank Didier Lemoine for helpful discussions regarding the IOS approximation and for performing initial close-coupling calculations. Finally, we thank William Klemperer, Fu-Ming Tao, and Kelly Higgins for sharing their HeClF data before publication and for many valuable discussions regarding this problem.

Note Added in Proof: We have recently become aware of the fact that McCourt and Naumkin (private communication) have also been fitting the potential energy surfaces discussed in this paper. They start with somewhat higher level *ab initio* points than we did and obtain good fits with minor adjustments. For $ArCl_2$, their results and ours are quite similar for the perpendicular well, for which the data are most sensitive, but McCourt and Naumkin were able to fit the data with a linear well whose position is closer to that of the *ab initio* points than for our fit. Their results and ours are quite similar for $NeCl_2$.

References and Notes

(1) Cline, J. I.; Evard, D. D.; Thommen, F.; Janda, K. C. *J. Chem. Phys.* **1986**, *84*, 1165.

(2) Cline, J. I.; Sivakumar, N.; Evard, D. D.; Janda, K. C. *Phys. Rev. A* **1987**, *36*, 1944.

(3) Cline, J. I.; Reid, B. P.; Evard, D. D.; Sivakumar, N.; Halberstadt, N.; Janda, K. C. *J. Chem. Phys.* **1988**, *89*, 3535.

(4) Beneventi, L.; Casavecchia, P.; Volpi, G. G.; Bieler, C. R.; Janda, K. C. *J. Chem. Phys.* **1993**, *98*, 178.

(5) Huang, S. S.; Bieler, C. R.; Tao, F.-M.; Klemperer, W.; Casavecchia, P.; Volpi, G. G.; Halberstadt, N.; Janda, K. C. *J. Chem. Phys.* **1995**, *102*, 8846.

(6) Reid, B. P.; Janda, K. C.; Halberstadt, N. *J. Chem. Phys.* **1988**, *92*, 587.

(7) Chałasiński, G.; Gutowski, M.; Szczęśniak, M. M.; Sadlej, J.; Scheiner, S. *J. Chem. Phys.* **1994**, *101*, 6800.

(8) Williams, J.; Rohrbacher, A.; Djahandideh, D.; Janda, K. C.; Jamka, A.; Tao, F.-M.; Halberstadt, N. *Mol. Phys.* **1997**, *91*, 573.

(9) Rohrbacher, A.; Williams, J.; Janda, K. C.; Cybulski, S. M.; Burcl, R.; Szczęśniak, M. M.; Chałasiński, G.; Halberstadt, N. *J. Chem. Phys.* **1997**, *106*, 2685.

(10) Grigorenko, B. L.; Nemukhin, A. V.; Apkarian, V. A. Submitted for publication in *J. Chem. Phys.*

(11) Brinza, D. E.; Swartz, B. A.; Western, C. M.; Janda, K. C. *J. Chem. Phys.* **1983**, *79*, 1541.

(12) Brinza, D. E.; Western, C. M.; Evard, D. D.; Thommen, F.; Swartz, B. A.; Janda, K. C. *J. Chem. Phys.* **1984**, *88*, 2004.

(13) Evard, D. D.; Thommen, F.; Janda, K. C. *J. Chem. Phys.* **1986**, *84*, 3630.

(14) Evard, D. D.; Thommen, F.; Cline, J. I.; Janda, K. C. *J. Phys. Chem.* **1987**, *91*, 2508.

(15) Cline, J. I.; Sivakumar, N.; Evard, D. D.; Bieler, C. R.; Reid, B. P.; Halberstadt, N.; Hair, S. R.; Janda, K. C. *J. Chem. Phys.* **1989**, *90*, 2605.

(16) Halberstadt, N.; Beswick, J. A.; Janda, K. C. *J. Chem. Phys.* **1987**, *87*, 3966.

(17) Buchachenko, A. A.; Stepanov, N. F. Submitted for publication in *J. Chem. Phys.*

(18) Evard, D. D.; Cline, J. I.; Janda, K. C. *J. Chem. Phys.* **1988**, *88*, 5433.

(19) Xu, Y.; Jäger, W.; Ozier, I.; Gerry, M. C. L. *J. Chem. Phys.* **1993**, *98*, 3726.

(20) Tao, F.-M.; Klemperer, W. *J. Chem. Phys.* **1992**, *97*, 440.

(21) Sadlej, J.; Chałasiński, G.; Szczęśniak, M. M. *J. Mol. Struct.*: *THEOCHEM* **1994**, *307*, 187.

(22) Halberstadt, N.; Serna, S.; Roncero, O.; Janda, K. C. *J. Chem. Phys.* **1992**, *97*, 341.

(23) Naumkin, F. Y.; Knowles, P. J. *J. Chem. Phys.* **1995**, *103*, 3392.

(24) Wang, F.; McCourt, F. R. W. *J. Chem. Phys.* **1996**, *104*, 9304.

(25) Beneventi, L.; Casavecchia, P.; Volpi, G. G. *J. Chem. Phys.* **1986**, *85*, 7011.

(26) Parker, G. A.; Pack, R. T. *J. Chem. Phys.* **1978**, *68*, 1585.

(27) Pack, R. T. *Chem. Phys. Lett.* **1978**, *55*, 197.

(28) Beneventi, L.; Casavecchia, P.; Volpi, G. G.; Wong, C. C. K.; McCourt, F. R. W.; Corey, G. C.; Lemoine, D. *J. Chem. Phys.* **1991**, *95*, 5827.

(29) Beneventi, L.; Casavecchia, P.; Vecchiocattivi, F.; Volpi, G. G.; Buck, U.; Lauenstein, Ch.; Schinke, R. *J. Chem. Phys.* **1988**, *89*, 4671.

(30) Beneventi, L.; Casavecchia, P.; Volpi, G. G. *Electronic and Atomic Collisions*; MacGillivray, W. R., McCarthy, I. E., Standage, M. C., Eds.: IOP Publishing, Ltd, Bristol, 1992; pp 527−536.

(31) Faubel, M.; Kohl, K. H.; Toennies, J. P. *J. Chem. Phys.* **1980**, *73*, 2506.

(32) Beneventi, L.; Casavecchia, P.; Vecchiocattivi, F.; Volpi, G. G.; Lemoine, D.; Alexander, M. H. *J. Chem. Phys.* **1988**, *89*, 3505.

(33) Gianturco, F. A.; Palma, A. *J. Phys. B* **1985**, *18*, L519. Battaglia, F.; Gianturco, F. A.; Palma, A. *J. Chem. Phys.* **1984**, *80*, 4997.

(34) Bowers, M. S.; Faubel, M.; Tang, K. T. *J. Chem. Phys.* **1987**, *87*, 5687.

(35) Beneventi, L.; Casavecchia, P.; Volpi, G. G.; Wong, C. C. K.; McCourt, F. R. W. *J. Chem. Phys.* **1993**, *98*, 7926.

(36) Evard, D. D. Ph.D. Thesis, California Institute of Technology, 1988.

(37) $D_0(NeCl_2) = 59.7 \pm 2.0$ cm^{-1} (ref 15) and $D_0(ArCl_2) = 187.9 \pm 1.0$ cm^{-1} (ref 36).

(38) For $HeCl_2$ values from a rigid-rotor fit to LIF spectra were used ($A = 0.31(5)$ cm^{-1}, $B = 0.2435$ cm^{-1}, and $C = 0.14(1)$ cm^{-1} (ref 3)). The values for $NeCl_2$ were from ref 14 ($A = 0.2435$ cm^{-1}, $B = 0.085(2)$ cm^{-1}, and $C = 0.063(1)$ cm^{-1}). The values $A = 0.245\,953(4)$ cm^{-1}, $B = 0.048\,169\,591(8)$ cm^{-1}, and $C = 0.040\,038\,128(7)$ cm^{-1} for $ArCl_2$ were obtained from microwave measurements.[19]

(39) Carroll, D. L. FORTRAN genetic algorithm (GA) driver, version 1.6.1, available at http://www.uiuc.edu/ph/www/carroll/ga.html.

(40) Lemoine, D. Private communication.

(41) Cockett, M. C. R.; Beattie, D. A.; Donovan, R. J.; Lawley, K. P. *Chem. Phys. Lett.* **1996**, *259*, 554.

(42) Klemperer, W.; Higgins, K.; Tao, F.-M. Private communication.

(43) Buck, U. *Atomic and Molecular Beam Methods*; Scoles, G., Ed.; Oxford University Press: Oxford, 1988; p 500.